



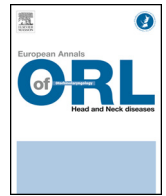
Since January 2020 Elsevier has created a COVID-19 resource centre with free information in English and Mandarin on the novel coronavirus COVID-19. The COVID-19 resource centre is hosted on Elsevier Connect, the company's public news and information website.

Elsevier hereby grants permission to make all its COVID-19-related research that is available on the COVID-19 resource centre - including this research content - immediately available in PubMed Central and other publicly funded repositories, such as the WHO COVID database with rights for unrestricted research re-use and analyses in any form or by any means with acknowledgement of the original source. These permissions are granted for free by Elsevier for as long as the COVID-19 resource centre remains active.



Available online at
ScienceDirect
www.sciencedirect.com

Elsevier Masson France
EM|consulte
www.em-consulte.com/en



Review

The influenza virus, SARS-CoV-2, and the airways: Clarification for the otorhinolaryngologist



L. de Gabory^{a,b,*}, A. Alharbi^a, M. Kérimian^a, M.-E. Lafon^c

^a Department of ENT and Head & Neck Surgery, Bordeaux University Hospital, France

^b University Bordeaux, 33000 Bordeaux, France

^c Department of Virology and Biological Monitoring Unit, Bordeaux University Hospital, France

ARTICLE INFO

Keywords:

Influenza virus
 SARS-CoV-2
 COVID-19
 Respiratory infection
 Airborne particle

ABSTRACT

The influenza virus and SARS-CoV-2 cause trivial upper and severe lower respiratory infections (Influenza virus 290,000 to 650,000 deaths/year). These viruses come into contact with the airways either by direct projection, by secondary inhalation of airborne droplets, or by handling (fomites). The objective of this article is to clarify the mechanisms of production and penetration of droplets of secretions emitted during all expiratory phenomena likely to transport these viruses and come into contact with the respiratory mucosa. The droplets $>5 \mu\text{m}$ follow the laws of ballistics, those $<5 \mu\text{m}$ follow Brownian motion and remain suspended in the air. The aerosols of droplets are very heterogeneous whether the subject is healthy or sick. During an infectious period, not all droplets contain viral RNA. If these RNAs are detectable around patients, on surfaces, and in the ambient air at variable distances according to the studies (from 0.5 m to beyond the patient's room), this is without prejudice to the infectious nature (viability) of the virus and the minimum infectious dose. There is a time lag between the patient's infectious period and that of RNA detection for both viruses. Subsequently, the inhaled particles must meet the laws of fluid dynamics (filtration) to settle in the respiratory tree. All of this partly explains the contagiousness and the clinical expression of these two viruses from the olfactory cleft to the alveoli.

© 2020 Elsevier Masson SAS. All rights reserved.

1. Introduction

Lower respiratory infections are the leading cause of death in poor countries and the 6th in high income countries (<https://www.who.int/news-room/fact-sheets/detail/the-top-10-causes-of-death>). Upper respiratory infections are the most frequent sources of morbidity with 2 to 5 colds/adult/year and 7 to 10 colds/infant/year [1,2]. Coronaviruses belong to the *Coronaviridae* family which has 4 genera: α - β - γ - δ . Genera α and β contain 7 coronaviruses transmissible to humans: Four are responsible for trivial upper and lower respiratory infections, the three others, SARS-CoV-1, MERS-CoV, and SARS-CoV-2 are responsible for severe lower respiratory infections [3]. They have an S surface glycoprotein (Spike) arranged like a crown which allows them to attach themselves to the epithelial receptor angiotensin-converting enzyme 2 (ACE2) and the protease transmembrane TRMPSS2 [4–8]. The A and B influenza viruses (IV) and the seasonal flu belong to the *Orthomyxoviridae* family and are responsible for

290,000 to 650,000 deaths/year worldwide through respiratory failure [9]. They have a haemagglutinin surface glycoprotein that attaches to sialic acid [10].

The inter-human transmission of viral infection occurs through close direct contact with an infected person, by touching a surface contaminated with short-distance projections, and impaction of droplets of secretion (fomites) [11]. Transmission can occur over a longer distance by airborne droplets [12,13]. The objective of this clarification was to analyse the objective data of patients' contagiousness by transporting the virus through producing secretions and the possibility of them penetrating the airways. Assessing transmissibility is important for the otorhinolaryngologist who is at the forefront of treating the upper aerodigestive tracts and because many viruses cause ENT manifestations. Finally, the current SARS-CoV-2 pandemic and the annual flu epidemic require professionals to be up to date with the latest knowledge about these mechanisms in order to adapt their practices.

2. Method

A structured search on PubMed was carried out until the end of April 2020. It took publications with abstracts in French and English into consideration. The terms searched were “influenza virus”,

* Corresponding author at: Department of ENT and Head & Neck Surgery, Bordeaux University Hospital, Pellegrin Hospital, Michelet Centre, place Amélie Raba-Léon, 33076 Bordeaux cedex, France.

E-mail address: ludovic.de-gabory@chu-bordeaux.fr (L. de Gabory).

“SARS-CoV2”, “COVID-19”, “transmission”, “respiratory infection”, “airborne particle”, “cough”, “sneezing”, “droplet”, “microparticle”, “nanoparticle”, “particle deposition”. References were added from relevant article references or from the authors’ names. After reading the title and abstract, the following studies were excluded: those with a mismatch between the objectives and the conclusion, duplicates, clinical cases, series <20 patients, literature reviews, and studies outside of the objectives (e.g. epidemiology/therapeutic). Letters to the editor and editorials were excluded except if they presented new experimental data. As an example, the term “COVID 19 AND transmission” returned 1292 publications while it exists only since December 2019: there were only 625 with an abstract. The following were excluded: 45 clinical cases, 38 editorials, 20 letters to the editor, and 148 literature reviews. The abstracts were analysed, and the article read in full before being selected or rejected. Internet references are given for explanatory purposes.

3. Discussion

The air that we breathe transports particles of different sizes (granulometry) (Table 1) combining pollution, diesel, allergens, and viruses [3,18,20,21]. Its composition varies depending on the place (indoors/outdoors, city/countryside), the day, meteorology (wind, hygrometry), profession, weeks, months, seasons, and countries [16,22–25]. Coughing, sneezing, or simply breathing and speaking produces thousands of droplets whose sizes vary from the microscale to the nanoscale (Table 1) [14]. The largest ones, > 5 μm , follow the laws of ballistics and of gravity. Their inertia parameter is defined as the product of the density (ρ) multiplied by the diameter of the particle squared (d^2) and the flow (Q) (Inertia parameter = $\rho d^2 Q$ in $\text{g}\cdot\mu\text{m}^2/\text{s}$) [26]. A droplet of 100 μm will settle on the ground in 16 s [27]. Finer particles, < 5 μm , make up the breathable part of the aerosol, remain airborne (negligible falling speed limit < 25 cm/s), and follow Brownian motion [28–31]. There are thus short-range or long-range particles depending on their capacity to remain airborne or not. On the other hand, from their creation, the droplets undergo evaporation (droplet nuclei) which reduces their diameter and increases their capacity to remain airborne, encouraging the maintenance of a long-range contamination source: a particle of 100 μm will take 100 seconds to reach a diameter of 32 μm in an atmosphere with 95% humidity, and less than 2 seconds in an atmosphere with 35% humidity. Inversely, evaporation can make other droplets with smaller diameters disappear [27,28,32].

Table 1
Size of the main particles likely to be inhaled.

Particles	Mean diameter	References
When calm expiration	0–500 μm	Xie 2009 [14], Tang 2013 [15]
When coughing	0–1500 μm	
Grasses (Timothy grass)	30–40 μm	Crouzy 2016 [16]
House dust mite	22 \pm 6 μm	Zhang 2019 [17]
Pollution		Lapuerta 2003 [18] Ezz 2015 [19]
PM10	< 10 μm	
Fines	< 2,5 μm	
Ultrafines	< 100 nm	
Virus		CSG 2020 [3]
Rhinovirus	28–30 nm	
Coronavirus	80–200 nm	
Influenza A & B	80–120 nm	
Syncytial Virus	150–400 nm	

3.1. Production, diffusion, and penetration of droplets from the patient to the recipient

3.1.1. During normal expiration and speech

The air that we breathe out through our nose or mouth is projected a distance of 0.6 to 0.8 m at an average maximum speed of 1.3 to 3.9 m/s [15,33]. Depending on the studies, the total number of droplets produced is estimated between 112 and 6720 droplets, when the subject is asked to count from 0 to 100 out loud. 90% settle on the ground at a distance of 30 cm [14]. Their size, however, is very heterogeneous and variable from one individual to another between 0 and 500 μm with an average diameter of 16 μm [14,33]. These droplets represent a mass of 18 to 79 mg [14]. More recently, Asadi et al. have demonstrated a production of 4.8 ± 3 particles/s with diameters of 0.5 to 5 μm while speaking, with a production rate that correlates with increasing voice loudness [34].

The digital simulation of droplets < 5 μm produced by normal expiration between two people face-to-face showed that, after 200 seconds, 6.2–5.7–0.8 and 0.4% settled on the subject facing them at respective distances of 0.5–1–1.5 and 3 metres [27]. The proportion of inhaled airborne droplets was 0.2–0.6–0.02 and 0% for the same distances [27]. The authors estimated the safe distance at 1.5 m [27]. This distance must be adjusted depending on oral or nasal breathing, the size of the people, the position of the face, the ambient humidity, the room’s ventilation, and the exposure time [27,34].

3.1.2. When sneezing and coughing

The average flow rate of a sneeze is 4.8 L/s, the air is projected 0.6 m at a maximum speed of 4.5 to 8 m/s with an expansion rate of 2 m^2/sec [15,35,36]. For coughing, the air is projected 0.7 m at a maximum speed of 6 to 11.7 m/s with an expansion rate of 1.5 m^2/sec [15,33,35]. It will be noted that these parameters are not very different [15].

In the healthy subject, who by definition does not cough, a cough would produce on average 800 to 2045 droplets with 80% settling on the ground at a distance of more than 50 cm [14,33]. When coughing, the granulometry of the droplets produced has a different distribution compared to that observed when speaking, with diameters ranging from 0 to 1500 μm . However, their average diameters are quite close: 13.5 μm for coughing versus 16 μm for speaking [14,33]. Their mass is between 23 and 85 mg after 20 successive coughs [14].

3.1.3. Which droplets can penetrate the airways?

Large droplets have little chance of reaching the recipient’s airways as these are short-range objects. Safe distances are useful even though they can vary twofold depending on the studies [20,27] and their contaminating properties have not been demonstrated (see below). Airborne droplets can reach the airways: in a calm environment, a 4 μm particle takes 33 minutes to move 1 metre and a 1 μm particle takes 8 hours. However, it must pass through the nasal filter whose filtration capacity is not linear [26]. On the microscale, the bigger the particle the more it is filtered. On the nanoscale, it is the reverse: the smaller the particle the more it is filtered [30,37]. For calm respiration (10–15 L/min), 100% of 20 μm particles settle in the nasal fossa and the cavum, 40% for 9 to 11 μm particles, and only 4% for those from 2.5 μm [31,38]. For the same flow rate, 80% of 1 nm particles settle in the nasal fossa, 40% of 4 nm particles, and 10% of those between 10 and 100 nm [30,37]. The deposit rate in the nasal fossa and the cavum is thus the same for particles from 20 μm and from 1 nm. However, as a result of the influence of the inertia parameter or of Brownian motion, the mapping of the deposits is different: particles from 20 μm will follow the main air current and will impact on anatomical structures in the back third of the nasal fossa where the flow changes direction, while particles from

Table 2
Deposit rate of particles inhaled during normal respiration obtained through digital simulation (18 L/min).

Deposition rate (%)	1 nm	10 nm	100 nm	1 μm	15 μm	100 μm
Nasal Fossa	49,8	8,1	6,9	3	23,2	100
Pharynx/larynx	11,6	4,9	4,7	1,1	1,4	0
Trachea	27,5	6,1	2,4	1,9	10,8	0
Lungs				94	61,6	0

Only 14% of 100 nm particles are stopped in the respiratory tree after inspiration [29,42].

1 nm will be deposited in all directions, all over the nasal mucosa [30,37,38].

Several variation factors play a part: when the density increases, the inertia parameter increases the capacity of microscale particles to impact while it has no effect on nanoscale particles [30]. An increasing airflow will have the same effect on the microscale, while it decreases the deposit rate of nanoscale particles, all the more so if they are smaller [30,38]. This behaviour for nanoscale particles is applicable throughout the nasal fossa except in the olfactory cleft, where this parameter is not modified or only slightly modified [37,39], which is very important for viruses transported by a large heterogeneity of airborne droplets (from 0.3 and 4 μm) [21,40]. After the inspiratory phase, the still airborne particles in reverse flow will increase their deposit rate in the nasal fossa and the olfactory clefts because of upwards air deflection by the turbinates, and increase their residence time through the resistance of the nasal valve [41].

In contrast, particles between 10 μm and 10 nm are not filtered by the nose and can penetrate the rest of the airways (Table 2). These filtration characteristics are already used in daily practice for aerosol therapy since it is recommended to use machines producing particles > 5 μm for rhinological pathologies, from 5 to 2 μm for tracheobronchial pathologies, and between 2 and 0.5 μm if intended for the pulmonary alveoli [43,44]. FFP-type respiratory protection masks are tested on inspiration and classed according to their filtration performance with regard to a sodium chloride aerosol composed of particles with a median diameter of 0.6 μm and a paraffin oil aerosol with a median diameter of 0.4 μm (www.inrs.fr/dms/inrs/CataloguePapier/ED/TI-ED-6106/ed6106.pdf), with 3 levels of protection: FFP1 the filter allows only 20% of the particles to penetrate on inspiration with a maximum leakage rate of 22% (interior leakage), FFP2 – the filter allows only 6% of the particles to penetrate with a maximum leakage rate of 8%, and FFP3 – where only 1% of the particles penetrate with a maximum leakage rate of 2%. The mechanisms for stopping the droplets vary depending on the granulometry: from 10 to 1 μm , the inertia parameter and gravity are used; from 1 μm to 300–100 nm, the number, diameter, and weave of the fibres allow for mechanical filtration; below this, the particles are retained by the electrostatic properties of the fibres and diffusion [45,46]. The performance of a mask is a compromise between the difficulty with breathing (pressure loss < 30 Pa) and its filtration capacity, which depends on fluid and electrostatic mechanics but also on their fitting to the face [45,46]. “Home-made” masks made of several fabrics (cotton/silk) and several layers (3 to 4) can match the performance of industrial masks [45], knowing that small-diameter fibres increase the electrostatic capture of nanoparticles [46].

3.2. Transmission of the influenza virus

During a flu, the air volume of a cough does not change before and after the illness and varies from 2.33 to 2.48 L/cough with a flow of 5.33 to 6.9 L/sec [21,47]. The number of particles on coughing varied widely from one individual to another: while ill, it was $75,400 \pm 97,300$ droplets/cough, and $52,200 \pm 98,600$ droplets/cough after recovery (non-significant difference). In contrast, the average volume via aerosol was 38.3 pL/cough while ill versus 26.4 pL/cough afterwards ($P < 0.0143$) [21]. The size of this aerosol's droplets varied little during and after the illness, between 0.35 to 2.5 μm for an average of 0.63 μm [21].

Gratton et al. showed, during coughing, the presence of IV, rhinovirus, and respiratory syncytial virus in 12 adults and 41 children, 57% of the particles were > 5 μm and 82% were < 5 μm [48]. Milton et al., with 33 patients, found that 43% of particles > 5 μm carried flu virus RNA, and 92% of particles < 5 μm did so [49]. The number of viral copies was only 12 copies/30 minutes in the coarse part of the aerosol while there was on average 560 copies/30 minutes in particles < 5 μm . Wearing a surgical mask reduced the risk of diffusion of viral copies by a factor of 25 for particles > 5 μm and by 2.8 times for particles < 5 μm [49].

In flu season and respiratory syncytial virus infection, Lindsley et al. measured the presence of airborne viral RNA in 264 samples taken from fixed stations and from 21 employees at a health-care facility treating patients suffering from both illnesses. These RNAs were detected in the air and there was a good correlation between the number of positive samples and the number of positive patients [20]. This was especially the case in poorly ventilated rooms such as examination rooms (door closed) where the concentration was at a maximum. These RNAs were contained in 43% of the particles with a diameter $\leq 4.1 \mu\text{m}$. The maximum of samples was positive in an area 1.8 m around the patient and for higher up stations because of the room's ventilation system, demonstrating these particles' capacity to remain airborne [20]. In other facilities, the virus was found airborne in patients' rooms only in 50% of cases with 162 ± 1.9 copies/ m^3 in 24% of particles > 4 μm , 144 copies/ m^3 in 6% of particles between 1–4 μm , and none in particles < 1 μm [40].

However, the presence of viral RNA does not imply contagiousness: what do these values mean? Does this represent an infectious risk for the individual? No statistically significant association was highlighted between the level of viral excretion and transmission [50,51]: finding viral RNA or a viral load is without prejudice to the viability of the virus and the minimal infectious dose. In a H1N1 and H3N1 IV infection model, it is the loss of positivity of the viral culture that signals the non-contaminant nature of the patient but not the absence of RNA, which coincides with the end of the infectious period. Alford et al. administered the IV to healthy volunteers in order to measure the minimal infectious dose [52]. Via aerosol distributing droplets of 1 to 3 μm , the infectious dose for humans was from 0.6 to 3 TCID₅₀/mL (dose necessary to infect 50% of the cells in a reference cell culture). Administered as nasal droplets, this value was from 127 to 320 TCID₅₀/mL [53]. Patients infected by the aerosol said that their symptoms were in line with the usual ones, while those infected by nasal inoculation had low-intensity symptoms over longer periods [52,53].

In practice, the percentage of infectious IV in droplets produced by coughing or expiration varied from 5 to 42% for particles from 0.3 to 8 μm in diameter where patients had clinical signs for 2 days [47,49,54,55]. Regardless, these figures vary widely depending on the granulometry of the particles. Lindsley et al. did not find infectious virus in particles > 5 μm [47]. In contrast, the quantity of infectious virus in airborne particles (< 5 μm) was enough to be contaminating [47,52]. However, these studies have low patient populations, involve mild forms of the illness, and do not take into account the kinetics of viral detection or the length of viability of the virus; their results depend on the sensitivity of the viral culture methods implemented to demonstrate infectivity. Lastly, the presence of infectious virus in expectoration does not mean that they will reach their target because these studies do not take into account distance and residence time, the environment (survival of IV A in low rates of hygrometry) [9], air movements, the

recipient's breathing, their sneezing, their mucociliary clearance, and their immune status.

3.3. Transmission of SARS-CoV-2

Guo et al. measured the presence of viral RNA in the air of Intensive Care Units (ICU) and traditional hospitalisation sections in Wuhan. The virus was present in 33% of the samples taken from near air treatment openings, in 44% of samples near patients, and in 12.5% of cases at the entrance to the ICU bedroom (4 m from the patient's head). The ground was systematically positive even outside of bedrooms, leading to half of employees' shoe soles being positive. In the hospitalisation sections, only 15.4% of samples were positive at 2.5 m from the patient's head, and 18.2% near the patient [56]. The presence of viral RNA followed human activity, air movements, and depended on the viral load of the patient, which is often more significant in ICU than in general hospitalisation where there are milder forms [57].

Yu F. et al. showed that, out of 323 samples taken from 76 confirmed COVID+ patients, the most productive biological liquids were, in descending order, spit, oropharyngeal swabs, and nasal swabs. Spit contained the most viral copies ($17,429 \pm 6920$ copies/test versus 2552 ± 1965 copies/test for oropharyngeal swabs, and 651 ± 501 copies/test for nasal swabs, $P < 0.001$) [58]. Other authors confirmed this result [59–61]: the viral load in saliva was very high the older than 60 the patients were, if they had 1 to 2 comorbidities, and/or a severe form in the first week. This salivary excretion of the virus seems to correlate with the biological markers of tissue damage and a strong expression of the ACE2 receptor in the oral mucosa [8,62]. However, others showed the superiority of nasopharyngeal swabs for diagnosing COVID-19 [63]. Given this heterogeneity of results, the American Centre for Disease Control and Prevention left the choice of the type of sample for diagnosing the illness to the discretion of the operator in its recommendations dated 26 April (<https://www.cdc.gov/coronavirus/2019-ncov/lab/guidelines-clinical-specimens.html>).

Zheng et al. demonstrated that, in 96 COVID+ patients, viral RNA was detected in respiratory secretions and stools up to the 3rd and 4th week after the onset of symptoms, with a net reduction in expression time for mild forms in comparison with severe forms [64]. These time periods were also found by others [60]. However, Xu et al. showed that, from a group of patients in Wuhan who had transmitted the virus to a group in another region, who themselves transmitted the illness to a third group, there was reduction in intensity and in the duration of RNA expression, which could indicate a finite phenomenon: the RNA was no longer detectable in samples taken from the third group 7 days after the onset of symptoms [60].

In any event, with the same tools used for the flu, the same questions are raised for SARS-CoV-2: is detecting viral RNA synonymous with contagiousness? If the viral RNA is detectable in respiratory secretions and stools after the clinical condition for more than a month, the "living" virus could not be detected by culture after the 3rd week: the results of the reverse transcription polymerase chain reaction (RT-PCR) remained positive 6 to 8 days after the loss of transmissibility [65]. He et al., with a contagiousness model for the flu and SARS-CoV-1 and using data from oropharyngeal samples taken from 77 COVID+ patients, estimated peak contagiousness at 2 days before and 1 day after the onset of symptoms, while viral RNA is detectable up to the 21st day after the onset of symptoms [66]. The experimental production of droplets $< 5 \mu\text{m}$ containing SARS-CoV-2 demonstrated the presence of viable virus in the aerosol for 3 hours at a temperature of $21\text{--}23^\circ\text{C}$ and in an atmosphere with 40% humidity [11]. The half-life of SARS-CoV-2 was estimated at

1 hour in air, < 1 hour on copper, 3.8 hours on cardboard, and 5.6 and 6.8 hours on stainless steel and plastic [11].

Finally, if the contamination modes are similar for IV and SARS-CoV-2, all of this data allows us to understand certain features and similarities in the clinical expression of the two viruses. Pneumopathies are common but for COVID+ patients, unlike the flu, inflammatory rhinological manifestations (congestion, nasal obstruction, and rhinorrhoea) are rare [67]. On the other hand, both viruses are capable of causing anosmia and ageusia, but the former is rare with associated rhinological inflammatory signs, slowly and slightly reversible, the latter is frequent, with little or no rhinological inflammatory signs but a quicker olfactory recovery of between 7 and 10 days [67,68]. For the flu, sialic acid is expressed on the surface of the ciliated epithelial cells [10]. For SARS-CoV-2, ACE2 and TRMPSS2 are expressed in the nasal mucosa and the olfactory mucosa [5–7]. However, mechanisms causing loss of function should not be similar as, in a population of 262 patients with flu-like symptoms, 70% of COVID+ patients (40 cases) manifested olfactory losses versus 17% of COVID- patients (35 cases) [69]. Other authors confirmed these results [68]. COVID+ patients with olfactory disorders were significantly younger than those who had none [68].

4. Conclusion

Droplets are produced during all expiratory phenomena in healthy and ill subjects with wide disparities between individuals and few between the two states. Aerosol droplets $< 5 \mu\text{m}$ seem to be the most problematic because they remain airborne. However, they do not all contain viral RNA. If viral RNA is detectable around patients, on surfaces, and in the surrounding air, this is without prejudice to the viability of the virus and the possibility of transmitting the illness. In this respect, there are a lot of similarities between IV and SARS-CoV-2. Finally, if droplets are inhaled, the minimal infectious dose must be reached. It is not known for SARS-CoV-2 and it is likely that contact time remains a determining factor.

This clarification should allow the ENT specialist to assess the situation in the professional contexts they encounter, to explain it to the general public, and to justify the necessary measures to take with discernment.

Funding

This work did not receive any specific funding.

Disclosure of interest

The authors declare that they have no competing interest.

References

- [1] Eccles R. Understanding the symptoms of the common cold and influenza. *Lancet Infect Dis* 2005;5:718–25.
- [2] Zambon MC, Stockton JD, Clewley JP, Fleming DM. Contribution of influenza and respiratory syncytial virus to community cases of influenza-like illness: an observational study. *Lancet* 2001;358:1410–6.
- [3] Coronaviridae Study Group of the International Committee on Taxonomy of Viruses. The species Severe acute respiratory syndrome-related coronavirus: classifying 2019-nCoV and naming it SARS-CoV-2. *Nat Microbiol* 2020;5(4):536–44.
- [4] Song W, Gui M, Wang X, Xiang Y. Cryo-EM structure of the SARS coronavirus spike glycoprotein in complex with its host cell receptor ACE2. *PLoS Pathog* 2018;14(8):e1007236.
- [5] Olender T, Keydar I, Pinto JM, Tatarsky P, Alkelai A, Chien MS, et al. The human olfactory transcriptome. *BMC Genomics* 2016;17:619.
- [6] Hoffman M, Kleine-Weber H, Schroeder S, Kruger N, Herrler T, Erichsen S, et al. SARS-CoV2 cell entry depends on ACE2 and TRMPSS2 and is blocked by a clinically proven protease inhibitor. *Cell* 2020;181:1–10.

- [7] Butowt R, Bilinska K. SARS-CoV-2: Olfaction, Brain Infection, and the Urgent Need for Clinical Samples Allowing Earlier Virus Detection. *ACS Chem Neurosci* 2020, <http://dx.doi.org/10.1021/acscchemneuro.0c00172>.
- [8] Xu H, Zhong L, Deng J, et al. High expression of ACE2 receptor of 2019-nCoV on the epithelial cells of oral mucosa. *Int J Oral Sci* 2020;12:8.
- [9] Iuliano AD, Roguski KM, Chang HH, Muscatello DJ, Palekar R, Tempia S, et al. Estimates of global seasonal influenza-associated respiratory mortality: a modelling study. *Lancet* 2018;391(10127):1285–300.
- [10] Shim JM, Kim J, Tenson T, Min JY, Kainov DE. Influenza Virus Infection, Interferon Response, Viral Counter-Response, and Apoptosis. *Viruses* 2017;9(8). [Pii E223].
- [11] van Doremalen N, Bushmaker T, Morris DH, Holbrook MG, Gamble A, Williamson BN, et al. Aerosol and Surface Stability of SARS-CoV-2 as Compared with SARS-CoV-1. *N Engl J Med* 2020;382(16):1564–7.
- [12] Booth TF, Kournikakis B, Bastien N, Ho J, Kobasa D, Stadnyk L, et al. Detection of airborne severe acute respiratory syndrome (SARS) coronavirus and environmental contamination in SARS outbreak units. *J Infect Dis* 2005;191(9):1472–7.
- [13] Chowell G, Abdirizak F, Lee S, Lee J, Jung E, Nishiura H, et al. Transmission characteristics of MERS and SARS in the healthcare setting: a comparative study. *BMC Med* 2015;13:210.
- [14] Xie X, Li Y, Sun HQ, Liu L. Expiratory droplets due to talking and coughing. *J R Soc Interface* 2009;6:703–14.
- [15] Tang JW, Nicolle AD, Klettner CA, Pantelic J, Wang L, Suhaimi AB, et al. Airflow dynamics of human jets: sneezing and breathing - potential sources of infectious aerosols. *PLoS One* 2013;8(4):e59970.
- [16] Crouzy B, Stella M, Konzelmann T, Calpini B, Clot B. All-optical automatic pollen identification: towards an operational system. *Atmos Environ* 2016;140:2020–212.
- [17] Zhang Y, Shang Y, Inthavong K, Tong Z, Sun B, Zhu K, et al. Computational investigation of dust mite allergens in a realistic human nasal cavity. *Inhal Toxicol* 2019;31(6):224–35.
- [18] Lapuerta M, Armas O, Gomez A. Diesel particle size distribution estimation from digital image analysis. *Aerosol Sci Tech* 2003;37:369–81.
- [19] Ezz WN, Mazaheri M, Robinson P, Johnson GR, Clifford S, He C, et al. Ultrafine Particles from Traffic Emissions and Children's Health (UPTeCH) in Brisbane, Queensland (Australia): study design and implementation. *Int J Environ Res Public Health* 2015;12(2):1687–702.
- [20] Lindsley WG, Blachere FM, Davis KA, Pearce TA, Fisher MA, Khakoo R, et al. Distribution of airborne influenza virus and respiratory syncytial virus in an urgent care medical clinic. *Clin Infect Dis* 2010;50(5):693–8.
- [21] Lindsley WG, Pearce TA, Hudnall JB, Davis KA, Davis SM, Fisher MA, et al. Quantity and size distribution of cough-generated aerosol particles produced by influenza patients during and after illness. *J Occup Environ Hyg* 2012;9(7):443–9.
- [22] Yamamoto N, Bibby K, Qian J, Hospodsky D, Rismani-Yazdi H, Nazaroff WW, et al. Particle-size distributions and seasonal diversity of allergenic and pathogenic fungi in outdoor air. *ISME J* 2012;6(10):1801–11.
- [23] Ribeiro H, Guimaraes F, Duque L, Noronha F, Abreu I. Characterisation of particulate matter on airborne pollen grains. *Environ Pollut* 2015;206:7–16.
- [24] Petrova VN, Russel CA. The evolution of seasonal influenza viruses. *Nat Rev Microbiol* 2018;16(1):47–60.
- [25] Ouyang Y, Yin Z, Li Y, Fan E, Zhang L. Associations among air pollutants, grass pollens, and daily number of grass pollen allergen-positive patients: a longitudinal study from 2012 to 2016. *Int Forum Allergy Rhinol* 2019;9(11):1297–303.
- [26] International Commission on Radiological Protection. Human Respiratory Tract Model for Radiological Protection. *Ann ICRP Publ* 1994;66(24):1–3 [<https://www.icrp.org/publication.asp?id=ICRP%20Publication%2066>].
- [27] Liu L, Li Y, Nielsen PV, Wei J, Jensen RL. Short-range airborne transmission of expiratory droplets between two people. *Indoor Air* 2017;27(2):452–62.
- [28] Nicas M, Nazaroff WW, Hubbard A. Toward understanding the risk of secondary airborne infection: emission of respirable pathogens. *J Occup Environ Hyg* 2005;2(3):143–54.
- [29] Inthavong K, Ge QJ, Li XD, Tu JY. Detailed predictions of particle aspiration affected by respiratory inhalation and airflow. *Atmos Environ* 2012;62:107–17.
- [30] Wang SM, Inthavong K, Wen J, Tu JY, Xue CL. Comparison of micron- and nanoparticle deposition patterns in a realistic human nasal cavity. *Respir Physiol Neurobiol* 2009;166(3):142–51.
- [31] Shang Y, Dong J, Inthavong K, Tu J. Comparative numerical modelling of inhaled micron-sized particle deposition in human and rat nasal cavities. *Inhal Toxicol* 2015;27(13):694–705.
- [32] Xie X, Li Y, Chwang ATY, Ho PL, Seto WH. How far droplets can move in indoor environments - revisiting the Wells evaporation-falling curve. *Indoor Air* 2007;17:211–25.
- [33] Chao CYH, Wan MP, Morawska L, Johnson GR, Ristovski ZD, Hargreaves M, et al. Characterization of expiration air jets and droplet size distributions immediately at the mouth opening. *J Aerosol Sci* 2009;40(2):122–33.
- [34] Asadi S, Wexler AS, Cappa CD, Barreda S, Bouvier NM, Ristenpart WD. Aerosol emission and superemission during human speech increase with voice loudness. *Sci Rep* 2019;9(1):2348.
- [35] Nishimura H, Sakata S, Kaga A. A new methodology for studying dynamics of aerosol particles in sneeze and cough using a digital high-vision, high-speed video system and vector analyses. *PLoS One* 2013;8(11):e80244.
- [36] Mortazavy Beni H, Hassani K, Khorramyeh S. In silico investigation of sneezing in a full real human upper airway using computational fluid dynamics method. *Comput Methods Programs Biomed* 2019;177:203–9.
- [37] Garcia G, Schroeter JD, Kimbell JS. Olfactory deposition of inhaled nanoparticles in humans. *Inhal Toxicol* 2015;27(8):394–403.
- [38] Schroeter JD, Tewksbury EW, Wong BA, Kimbell JS. Experimental measurements and computational predictions of regional particle deposition in a sectional nasal model. *J Aerosol Med Pulm Drug Deliv* 2015;28(1):20–9.
- [39] Schroeter JD, Kimbell JS, Asgharian B. Analysis of particle deposition in the turbinate and olfactory regions using a human nasal computational fluid dynamics model. *J Aerosol Med* 2006;19(3):301–13.
- [40] Leung NHL, Zhou J, Chu DKW, Yu H, Lindsley WG, Beezhold DH, et al. Quantification of Influenza Virus RNA in Aerosols in Patient Rooms. *PLoS ONE* 2016;11(2) [e0148669].
- [41] de Gabory L, Reville N, Baux Y, Boisson N, Bordenave L. Numerical simulation of two consecutive nasal respiratory cycles: toward a better understanding of nasal physiology. *Int Forum Allergy Rhinol* 2018;8(6):676–85.
- [42] Dong J, Shang Y, Tian L, Inthavong K, Qiu D, Tu J. Ultrafine particle deposition in a realistic human airway at multiple inhalation scenarios. *Int J Numer Method Biomed Eng* 2019;35(7):e3215.
- [43] Dautzenberg B, Becquemin MH, Chaumuzeau JP, Diot P. Bonnes pratiques de l'aérosolthérapie par nébulisations. *Rev Mal Respir* 2007;24:751–7.
- [44] Corcoran TE, Niven R, Verret W, Dilly S, Johnson BA. Lung deposition and pharmacokinetics of nebulized cyclosporine in lung transplant patients. *J Aerosol Med Pulm Drug Deliv* 2014;27(3):178–84.
- [45] Konda A, Prakash A, Moss GA, Schmoldt M, Grant GD, Guha S. Aerosol Filtration Efficiency of Common Fabrics Used in Respiratory Cloth Masks. *ACS Nano* 2020, <http://dx.doi.org/10.1021/acsnano.0c03252>.
- [46] Woon Fong Leung W, Sun Q. Electrostatic Charged Nanofiber Filter for Filtering Airborne Novel Coronavirus (COVID-19) and Nano-aerosols. *Sep Purif Technol* 2020;116886, <http://dx.doi.org/10.1016/j.seppur.2020.116886>.
- [47] Lindsley WG, Noti JD, Blachere FM, Thewlis RE, Martin SB, Othumpangat S, et al. Viable influenza A virus in airborne particles from human coughs. *J Occup Environ Hyg* 2015;12(2):107–13.
- [48] Gralton J, Tovey ER, McLaws ML, Rawlinson WD. Respiratory virus RNA is detectable in airborne and droplet particles. *J Med Virol* 2013;85(12):2151–9.
- [49] Milton DK, Fabian MP, Cowling BJ, Grantham ML, McDevitt JJ. Influenza virus aerosols in human exhaled breath: Particle size, culturability, and effect of surgical masks. *PLoS Pathog* 2013;9(3):e1003205.
- [50] Tsang TK, Fang VJ, Chan K-H, Ip DKM, Leung GM, Peiris JSM, et al. Individual Correlates of Infectivity of Influenza A Virus Infections in Households. *PLoS ONE* 2016;11(5) [e0154418].
- [51] Tsang TK, Cowling BJ, Fang VJ, Chan KH, Ip DK, Leung GM, et al. Influenza A Virus Shedding and Infectivity in Households. *J Infect Dis* 2015;212(9):1420–8.
- [52] Alford RH, Kasei JA, Gerone PJ, Knight V. Human influenza resulting from aerosol inhalation. *Pros Soc Exp Biol Med* 1966;122(3):800–4.
- [53] Douglas RG. Influenza in man. In: Kilbourne ED, editor. *The influenza viruses and influenza*. New York: Academic Press; 1975. p. 375–447.
- [54] Hatagishi E, Okamoto M, Ohmiya S, Yano H, Hori T, Saito W, et al. Establishment and clinical applications of a portable system for capturing influenza viruses released through coughing. *PLoS One* 2014;9(8):e103560.
- [55] Lindsley WG, Blachere FM, Beezhold DH, Thewlis RE, Noorbakhsh B, Othumpangat S, et al. Viable influenza A virus in airborne particles expelled during coughs versus exhalations. *Influenza Other Respir Viruses* 2016;10(5):404–13.
- [56] Guo ZD, Wang ZY, Zhang SF, Li X, Li L, Li C, et al. Aerosol and Surface Distribution of Severe Acute Respiratory syndrome Coronavirus 2 in Hospital Wards, Wuhan, China, 2020. *Emerg Infect Dis* 2020;26(7), <http://dx.doi.org/10.3201/eid2607.200885>.
- [57] Liu Y, et al. Viral dynamics in mild and severe cases of COVID-19. *Lancet Infect Dis* 2020, [http://dx.doi.org/10.1016/S1473-3099\(20\)30232-2](http://dx.doi.org/10.1016/S1473-3099(20)30232-2).
- [58] Yu F, Yan L, Wang N, Yang S, Wang L, Tang Y, et al. Quantitative Detection and Viral Load Analysis of SARS-CoV-2 in Infected Patients. *Clin Infect Dis* 2020, <http://dx.doi.org/10.1093/cid/ciaa345> [pii: ciaa345].
- [59] To KK, Tsang OT, Leung WS, Tam AR, Wu TC, et al. Temporal profiles of viral load in posterior oropharyngeal saliva samples and serum antibody responses during infection by SARS-CoV-2: an observational cohort study. *Lancet Infect Dis* 2020, [http://dx.doi.org/10.1016/S1473-3099\(20\)30196-1](http://dx.doi.org/10.1016/S1473-3099(20)30196-1) [pii: S1473-3099(20)30196-1].
- [60] Xu T, Chen C, Zhu Z, Cui M, Chen C, Dai H, et al. Clinical features and dynamics of viral load in imported and non-imported patients with COVID-19. *Int J Infect Dis* 2020, <http://dx.doi.org/10.1016/j.ijid.2020.03.022> [pii: S1201-9712(20)30141-7].
- [61] Ling Y, Xu SB, Lin YX, Tian D, Zhu ZQ, et al. The persistence and clearance of viral RNA in 2019 novel coronavirus disease survivors. *Chinese Med J* 2020, <http://dx.doi.org/10.1097/CM9.0000000000000774>.
- [62] Azzi L, Carcano G, Gianfagna F, Grossi P, Gasperina D, Genoni A, et al. Saliva is a reliable tool to detect SARS-CoV-2. *J Infect* 2020, <http://dx.doi.org/10.1016/j.jinf.2020.04.005> [pii: S0163-4453(20)30213-9].
- [63] Wang X, Tan Li, Wang X, Liu W, Lu Y, Cheng L, et al. Comparison of nasopharyngeal and oropharyngeal swabs for SARS-Cov-2 detection in 353 patients received tests with both specimens simultaneously. *Int J Infect Dis* 2020;94:107–9.
- [64] Zheng S, Fan J, Yu F, Feng B, Lou B, Zou Q, et al. Viral load dynamics and disease severity in patients infected with SARS-CoV-2 in Zhejiang province, China, January–March 2020: retrospective cohort study. *BMJ* 2020;369, <http://dx.doi.org/10.1136/bmj.m1443> [m1443].
- [65] Chan KH, Poon LL, Cheng VC, Guan Y, Hung IFN, Konget J, et al. Detection of SARS coronavirus in patients with suspected SARS. *Emerg Infect Dis* 2004;10:294–9.

- [66] He X, Lau EHY, Wu P, Deng X, Wang J, Hao X. Temporal dynamics in viral shedding and transmissibility of COVID-19. *Nat Med* 2020, <http://dx.doi.org/10.1038/s41591-020-0869-5>.
- [67] Giacomelli A, Pezzati L, Conti F, Bernacchia D, Siano M, Oreni L, et al. Self-reported olfactory and taste disorders in SARS-CoV-2 patients: a cross-sectional study. *Clin Infect Dis* 2020, <http://dx.doi.org/10.1093/cid/ciaa330> [pii: ciaa330].
- [68] Beltrán-Corbellini Á, Chico-García JL, Martínez-Poles J, Rodríguez-Jorge F, Natera-Villalba E, Gómez-Corral J, et al. Acute-onset smell and taste disorders in the context of Covid-19: a pilot multicenter PCR-based case-control study. *Eur J Neurol* 2020, <http://dx.doi.org/10.1111/ene.14273>.
- [69] Yan CH, Faraji F, Prajapati DP, Boone CE, DeConde AS. Association of chemosensory dysfunction and Covid-19 in patients presenting with influenza-like symptoms. *Int Forum Allergy Rhinol* 2020, <http://dx.doi.org/10.1002/alr.22579>.